Supporting Information for

Staged self-assembly of colloidal metastructures

Qian Chen,[†] Sung Chul Bae,[†] and Steve Granick[*,†,‡,§]

† Department of Materials Science and Engineering, ‡Department of Physics, and

§Department of Chemistry, University of Illinois, Urbana, Illinois 61801, United States

Contents

Experimental Section

1. Particle monolayer preparation

A closely-packed monolayer of 1 μm red fluorescent sulfated latex particles (F-8851, Invitrogen Inc.) is deposited on a silicon wafer substrate using a reported method.[1d] In brief, 80 μL water/ethanol dispersion (volume ratio 1:1) containing 8 wt% latex particles in deionized (DI) water is dropped onto the top surface of a 1 cm × 1 cm piece of silicon wafer (pretreated by Piranha solution) surrounded by DI water located at the midbottom of a Petri dish. The dispersion spreads freely on the water surface until it covers nearly the entire area. Then 10 μL of sodium dodecyl sulphate (2 wt% in DI water) solution is added to the water surface to reduce the surface tension and condense the particles into a closely packed monolayer about 16 cm^2 in area. A silicon wafer (1.5 cm × 2.5 cm, pretreated by Piranha solution) is used to pick up a floating monolayer of particles, left to dry for later treatment. We find that this type of closely-packed monolayer can ensure high transfer efficiency in the later "stamping" step.

2. Deposition of gold patches

The ACB triblock colloids are made following another earlier report.[5b] In short, first the particle monolayer was coated with 2 nm of titanium, and 15 nm of gold, using a Temescal e-beam evaporation system. Particles were then lifted from the substrate with a polydimethylsiloxane (PDMS) stamp. PDMS stamps were prepared by mixing Sylgard 184 agents (Dow Corning) with monomer and cross-linking agent at weight ratio 10:1. Just before stamping, the PDMS surface was treated by oxygen plasma to induce necessary adhesion and wettability. The oxygen plasma was generated by a Harrick PDC-

32G plasma cleaner. A typical experiment used low plasma power, 6.8 W, chamber pressure around 150 mTorr, and treatment duration 50 sec. The stamp was then peeled off and used as the substrate for a second identical round of titanium and gold deposition. At this point both hemispheres of the particles have been coated, with thicker caps near the poles that gradually thin from the pole to the equator.

3. Gold etching to make ACB triblock colloids

We used a chemical gold etching solution to etch away the gold patches to reveal the middle, negatively charged C band. Gold etching solution was made using 4.93 g $Na_2S_2O_3$, 0.0867 g $K_4Fe^{II}(CN)_6$, 0.667 g $K_3Fe^{III}(CN)_6$, 11.2 g KOH, and 200 mL of deionized water. For the ACB triblock spheres we made, we use 70 sec of etching time to produce an A patch with 60° and a B patch with 40° half opening angle. This asymmetric patch decoration is enabled by the fact that the PDMS stamp protects from reaction the patch that presses into it. Finally, *n*-octadecanethiol (Sigma-Aldrich) was allowed to deposit on the particles, still sitting on the PDMS stamp after the etching step, from its 2 mM ethanol solution. After 2 hr, particles were first rinsed with 10 N HCl in their ethanol solution (volume ratio 1:50), then three times with ethanol, and harvested by ultrasonication in DI water.

4. Optical imaging

Optical micrographs illustrated in Figures 2 and 3 were observed by epifluorescence microscopy (63× air objective with a 1.6× post magnification, N. A. = 0.75). Images were captured by a ProEM electron multiplying charge coupled device (EMCCD) camera from Princeton Instruments.

Confocal laser scanning microscopy images as shown in Figure S4 were obtained using a Zeiss LSM LIVE7 system with 100x oil-immersion objective lens and 488 nm excitation.

Supplementary discussion

1. Comparison of self-assembly strategies

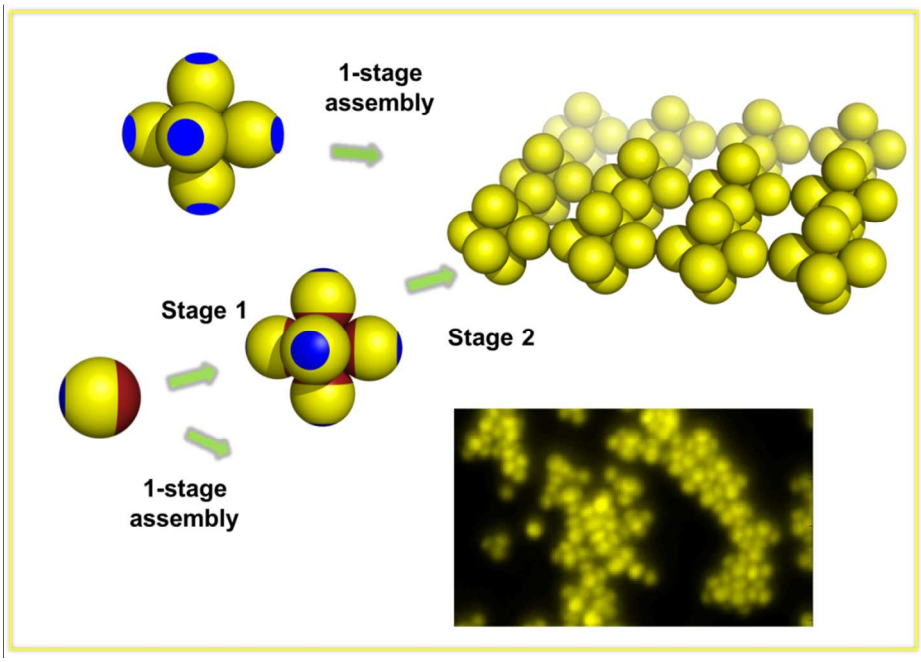

Figure S1: Schematic diagrams contrasting 1-stage assembly (top route) with staged assembly (middle route) in their effectiveness to form a "square lattice" wherein each lattice site is occupied by an octahedral cluster. Staged assembly greatly improves the efficiency. The bottom route illustrates that when all patchy attractions are activated at the same time (1-stage assembly), the assembled structure (fluorescence microscopic image) contains numerous imperfections.

2. Calculation of effective patch size

(i) Charge decoration of the spheres

A bare polystyrene sphere is modeled numerically with a uniform spherical surface coating of 8192 fixed and evenly distributed charged "nanoparticles." This number is chosen arbitrarily to render the "nanoparticle" size small relative to particle size (~1% the particle diameter). On the basis of specifications provided by the manufacturer, the surface charge density σ is 2.8 μC/cm^2. Accordingly, each nanoparticle (NP) has a charge $q = \frac{\sigma \times 4\pi r^2}{8192}$, q = 67.1 e. (elementary charge). The "triblock" characteristic is introduced by changing the charge of those NPs that reside within triblock surface domains.

(ii) The pair-wise interaction potential

The electrostatic potential between two triblock spheres at a fixed separation of 1.5 nm is calculated by summing pairwise NP-NP pair interactions, with the assumption that neither interferences nor correlations influence the potential between neighboring NPs. This approach follows in spirit an earlier study by one of the authors: Hong, L; Cacciuto, A.; Luijten, E; Granick, S. *Nano Lett.* **2006**, *6*, 2510. The NPs on interacting colloids interact via a screened Coulomb form (Yukawa potential):

$$V_E(i,j,I) = \frac{Z_i^{eff} Z_j^{eff}}{4\pi\varepsilon_o\varepsilon_r D_{ij}} \exp(-\frac{D_{ij}}{\lambda_D(I)})$$

where Z_i^{eff}, Z_j^{eff} are the effective charges, usually estimated as

$$Z^{eff} = Z\exp(\frac{R}{\lambda_D}) / (1+\frac{R}{\lambda_D})$$

for point charge-point charge pairs, $R = 0$, $Z^{eff} = Z$, so

$$V_E(i,j,I) = \frac{q_i q_j}{4\pi\varepsilon_o\varepsilon_r D_{ij}}\exp(-\frac{D_{ij}(\theta)}{\lambda_D(I)}) = \frac{q_i q_j \lambda_B}{D_{ij}}\exp(-\frac{D_{ij}(\theta)\sqrt{I/(M)}}{0.304})(k_B T)$$

where λ_B is the Bjerrum length, 0.7 nm in water, V_E is expressed in the unit of $k_B T$, and $D_{ij}(\theta)$ is the distance between NP pair of interest. Here, θ is the instantaneous in-plane tilt angle of the neighboring particles when A-A, A-B, or B-B patches on the two spheres initially share the same polar axis (Figure S2). Then the total pairwise potential is $V_E = \sum_{i,j} V_E(i,j)$.

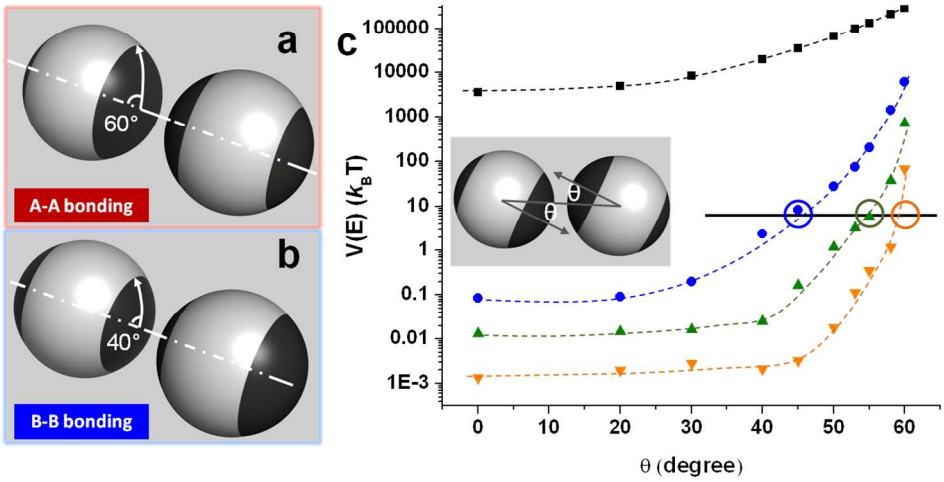

Figure S2: Pairwise electrostatic potential of two triblock spheres in close proximity. (**a**) and (**b**): two representative bonding schemes showing the axis-joining particle centers

intersecting the patch centers with A-A bonding (**a**), where the A patch has a half opening angle of 60°, and B-B bonding (**b**), with patch size of 40°. (**c**) Determination of the effective patch size θ_{eff} for A-A bonding at different ionic strengths: 0.01 mM (black squares), 0.2 mM (blue circles), 1 mM (green triangles), 5 mM (orange triangles). Here, θ_{eff} is defined as the orientation at which the electrostatic potential V(E) = 7 k_BT (the black flat line) is fully offset by one hydrophobic contact to produce zero total interaction. In the graph, these points are circled. The θ_{eff} increases with increasing ionic strength.

(iii) The effective patch size

The orientation θ at which the repulsion is fully offset by one hydrophobic contact, assumed to be $7\,k_BT$, is defined and calculated as θ_{eff} introduced in Figure 1b. In experiments, efforts are made to first exhaust A-A bonding, then to initiate B-B bonding at a considerably higher ionic strength with minimal side reaction of A-B bonds.

3. Distribution of small clusters formed at the first stage

This distribution shows the probability to find a certain cluster shape at the end of the first stage.

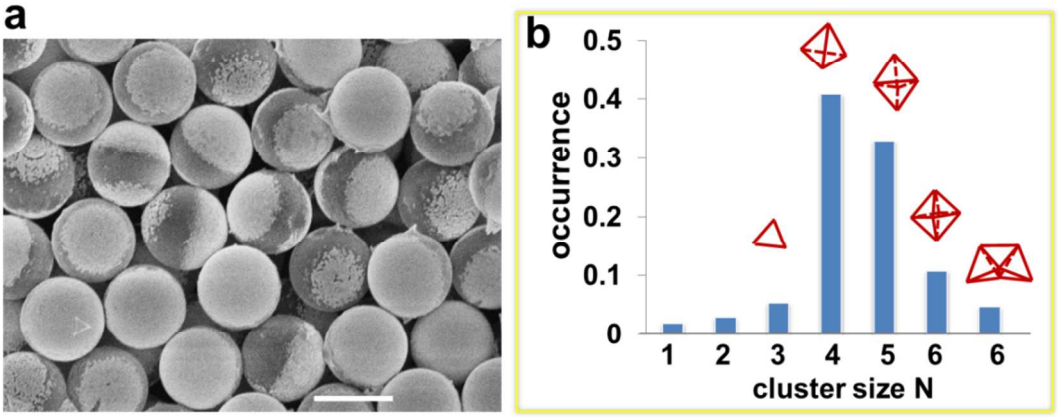

Figure S3: (**a**) Scanning electron microscopic (SEM) image of fabricated ACB triblock spheres. The brighter zones are gold patches. The darker zones are negatively charged polystyrene surfaces. Scale bar is 1 μm. Measured in terms of opening angle, the patch size is uniform within an uncertainty of less than 5°. (**b**) Shape distribution of clusters after equilibration subsequent to adding salt. Relative to the simpler AC Janus particles that we reported in an earlier study,[11] here the distribution shifts to smaller clusters because the A patch size is smaller than in that study. The distribution stabilizes 20 min after adding salt. When one waits even longer, the component particles within clusters continue to jiggle around with occasional rearrangements.

4. Final assembled structures

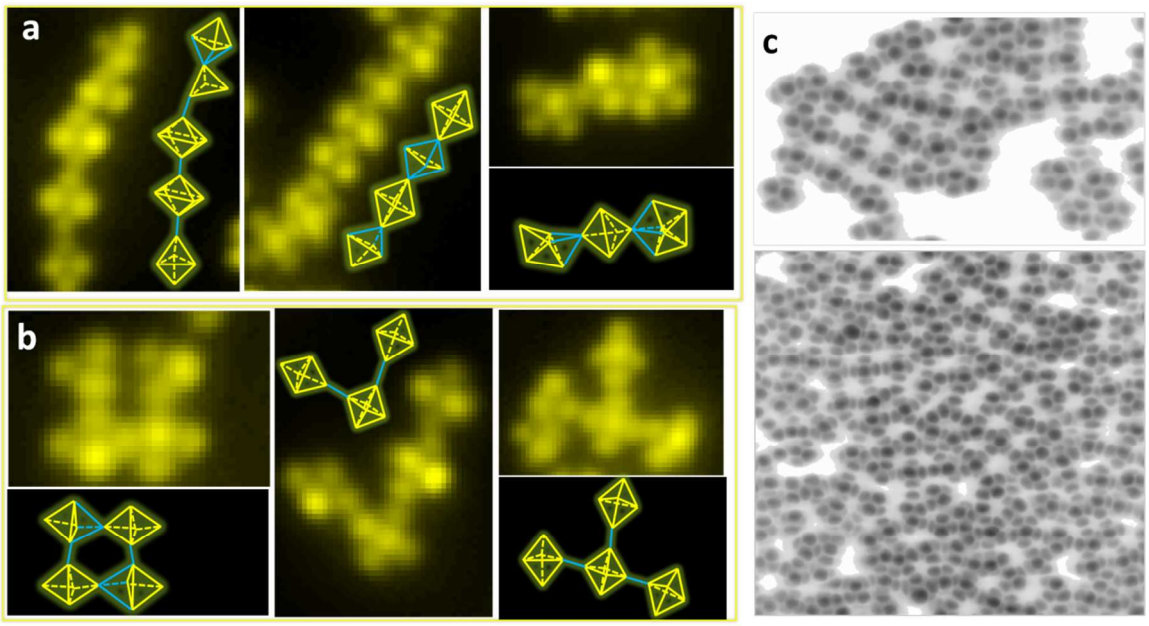

Figure S4: Typical structures after equilibration. From data of this kind, we obtained the statistics of connection schemes tallied in Table 1. (**a**) and (**b**): Fluorescence images of chain-like structures (**a**) and structures with right angles (**b**). Yellow lines show the bonds formed at the first stage, blues lines at the second stage. Structures with neighboring blue lines have A-B bonding at the second stage of assembly. (**c**) Confocal microscopy images of the tessellation of small clusters over the whole surface. The grey length scale was chosen to show the fluorescence intensity from a reconstructed 3D image from stacks of z scans. The networks formed by interconnected clusters are obvious visually.

5. Step-growth polymerization

Here we follow Figure 1 in ref 13 for definitions:

$N_{monomer}$: the number of small clusters, which is the analogue of monomers;

x-mer: an assembly structure composed of x monomers, which is an analogue of oligomers;

$\sum N_x$: the total number average of x-mers;

Figure 3 shows two quantitative analyses supporting the argument that triblock spheres assemble via step-growth polymerization :

First, the number-average degree of polymerization grows linearly with time (middle plot on the right); this is characteristic of reaction-controlled step-growth polymerization, in which the reactivity of functional groups of the monomers is independent of the chain length.

Second, probability of finding a x-mer: $N_x/N=(1-p)p^{x-1}$, where p is the reaction probability. Then we expect a linear relation of $\ln(N_x/N)$ versus (x-1): $\ln(N_x/N)= (x-1)\ln[(1-p)p]$, which is the bottom graph of Figure 3.

Supplementary movies

Movie S1. Fluorescence microscopy movie illustrating first-stage assembly after adding 1.2 mM NaCl to triblock spheres in deionized water. The volume fraction of particles close to the bottom surface is around 30%. Time is 3 times faster than real time.

Movie S2. Fluorescence microscopy movie showing second-stage assembly after adding additional NaCl to produce a final 5 mM concentration. Time is 3 times faster than real time.